Phase-Transition Optical Activity in Chiral Metamaterials

Fei Xie,[1] Mengxin Ren,[1,2,*] Wei Wu,[1] Dianqiang Yu,[1] Wei Cai,[1] and Jingjun Xu[1,†]
[1]The Key Laboratory of Weak-Light Nonlinear Photonics, Ministry of Education, School of Physics and TEDA Applied Physics Institute, Nankai University, Tianjin 300071, People's Republic of China
[2]Collaborative Innovation Center of Extreme Optics, Shanxi University, Taiyuan, Shanxi 030006, People's Republic of China

(Received 8 May 2020; accepted 29 September 2020; published 30 November 2020)

Optical activity from chiral metamaterials is both fundamental in electrodynamics and useful for polarization control applications. It is normally expected that due to infinitesimally small thickness, two-dimensional (2D) planar metamaterials cannot introduce large optical rotations. Here, we present a new mechanism to achieve strong optical rotation up to 90° by evoking phase transition in the 2D metamaterials through tuning coupling strength between meta-atoms. We analytically elucidate such phenomenon by developing a model of phase-transition coupled-oscillator array. And we further corroborate our ideas with both numerical simulations and experiments. Our findings would pave a new way for applying the concept of phase transition in photonics for designing novel optical devices for strong polarization controls and other novel applications.

DOI: 10.1103/PhysRevLett.125.237401

Chirality is a fundamental concept for the fact that it relates to the broken mirror symmetry and it has important implications in many areas of science [1–3]. Centuries ago, Arago [4] and Pasteur [5] successfully discovered a connection between the chirality and optical activity effect which causes rotation of light polarization azimuth while passing through the chiral media. Since then the chiro-optical interactions have attracted tremendous research interest in areas such as polarization control [6,7], nonlinear frequency conversion [8], chiro-optical spectroscopy [9,10], photonic topological insulators [11,12], and so on. However, the chiro-optical interactions are very weak in natural materials, thus how to enhance such response has become a research hot spot [13,14].

Recently, the emergence of metamaterials has provided a promising framework to achieve the significant chiro-optical response from subwavelength scales [15–17]. Mimicking the inherent three-dimensional (3D) feature of natural molecules, strong optical activity with optical rotation (ϕ) as high as 90° was achieved from 3D metamaterials [18–22] making of such as plasmonic helix [23–26], gyroid [27,28], and multilayered twisted nanostructures [1,29–33] *et al.* However, the 3D fabrication is highly challenging, particularly for optical metamaterials [34]. On the other hand, single layered metamaterials with subwavelength thickness are much easier to fabricate. Nevertheless, because of the infinitesimally short interaction length of light, they are generally considered to show weak optical rotation, and ϕ of only several degrees were normally observed for a long period of time [35–37]. In order to get stronger ϕ from the 2D metamaterials, dominant strategies adopted before were to optimize the individual meta-atom designs or evoke extrinsic chirality by oblique incidence [38–43]. Following such approaches, the optical chiral responses from individual meta-atoms could be boosted efficiently, but the ϕ still did not exceed 45° to the best of our knowledge [44–46].

A new mechanism to further increase the ϕ from the 2D metamaterials, preferably up to 90°, is needed. Such an effect holds primary potential for realizing polarization components with nanoscale dimensions, which is highly needed in various modern applications, such as microscopy, spectroscopy, displays, and telecommunication, etc. Here, we demonstrate a novel solution based on a concept of "phase transition." The phase transition is ubiquitous in nature and shows great importance in many branches of science including physics, chemistry, biology, and even sociology [47]. A distinct feature of the phase transition is that a tiny variation in control parameters near transition point would result in qualitatively different properties of the system. Thus, the phase transition provides a fascinating ability to achieve exotic properties from materials or systems by transforming them from one phase to another. For example, in electronics, various topological phase transitions have been observed in low temperature by imposing strong external magnetic field or spin-orbit coupling, which enable such as integer quantum Hall effect, fractional quantum Hall effect or topological insulators [48]. The phase transitions have been observed in photonic systems as well. Examples include abrupt increases in phase retardation of transmission from the metamaterials [49–51], changes between topological trivial and nontrivial states in photonic crystals [52], transition

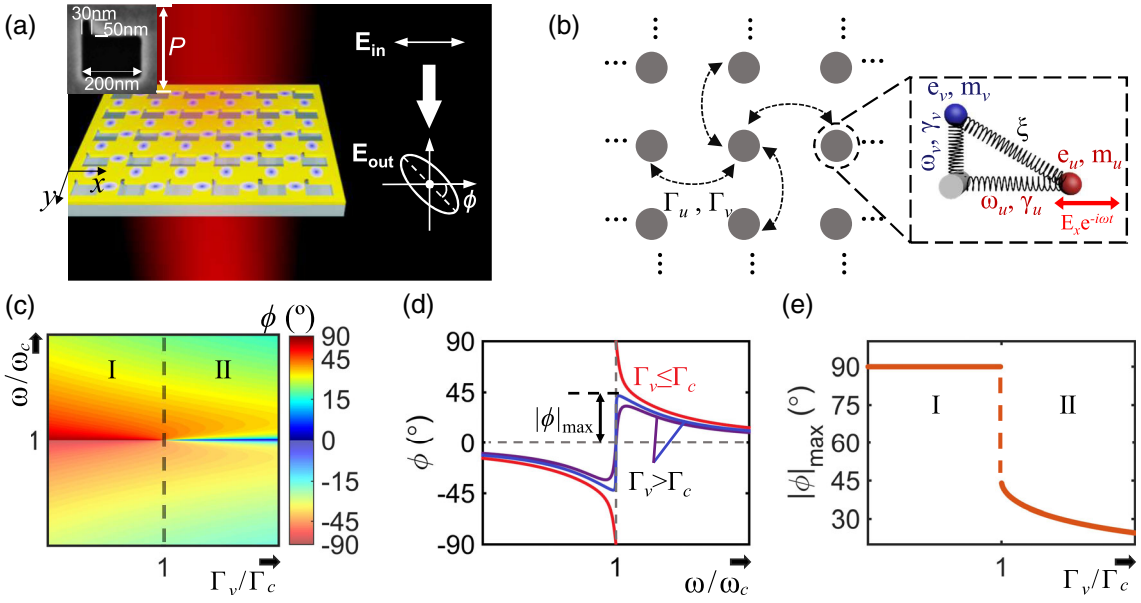

FIG. 1. Schematics of chiral metamaterial and phase-transition coupled-oscillator model. (a) Illustration of optical activity from the metamaterial array. Polarization rotation angle ϕ is positive for clockwise rotation when observed against the propagation direction. The inset shows SEM image of a single meta-atom with $P = 300$ nm. (b) Each meta-atom is represented by a dot, which consists of a charged coupled u- and v-oscillator pair with charges (e_u, e_v), masses (m_u, m_v), eigenfrequencies (ω_u, ω_v), and damping constants (γ_u, γ_v), respectively. They are mutually coupled by a third spring ξ. The response of any meta-atom is affected by its neighbors, which are denoted by Γ_u and Γ_v (corresponding to couplings between the u-u and v-v oscillators, respectively). (c) Phase diagram of the coupled-oscillator array as functions of Γ_v and ω. ϕ values are normalized within $(-90°, +90°]$. Two phases are labeled as I and II, depending on whether or not ϕ could achieve 90°. (d) Optical frequency ω dependence of ϕ, which achieves 90° for $\Gamma_v \leq \Gamma_c$. (e) Maximum achievable $|\phi|_{\max}$ is defined as an order parameter of the system, and its dependence on Γ_v shows an abrupt change at Γ_c, demonstrating the occurrence of the phase transition. The parameters for plotting (c)–(e) are $\omega_v = 0.4$ eV, $\gamma_v = 0.05$ eV, $\xi = 0.3$ eV^2 (refer to Supplemental Material [59] for details).

from the photonic crystals to the metamaterials [53], and observation of PT-symmetry phase transition around exceptional points in nanostructures [54], and so on.

In this Letter, we demonstrate the phase transition in the chiral metamaterials and the resulting abrupt increase in the optical activity. We would show that when inter-meta-atom couplings are reduced below a certain threshold, the metamaterials would enter a new phase, in which the 90° polarization rotation is achieved. "L"-shaped chiral metamaterials are used in our work. And a theoretical model based on a coupled-oscillator array, considering both the intra- and inter-meta-atom interactions, was developed to analytically elucidate such phase transition behaviors of the metamaterials. Furthermore, our ideas are corroborated by both numerical simulations and experimental results. Our results could find applications in flexible design of the ultracompact chiral optical devices for various applications.

The "L"-shaped meta-atoms, consisting of two dissimilar arms, on its own show chiral symmetry and would introduce the polarization azimuth rotation to incident light, as indicated in Fig. 1(a). The optical responses of the "L"-shaped meta-atoms could be intuitively understood based on a Born-Kuhn model [55–58], which consists of an array of coupled charged oscillators, as shown in Fig. 1(b). The u and v oscillators represent the two arms of the "L" meta-atoms, and they are constrained to move only along x or y axes, respectively. The resonant frequencies (ω_u, ω_v) and damping constants (γ_u, γ_v) of the two oscillators are different, respectively. Furthermore, the two oscillators are bounded to each other by a third spring with coupling constant ξ. Such oscillator system is chiral in symmetry, because it does not coincide with its mirror image. When x-polarized light ($E_x e^{-i\omega t}$) strikes the meta-atoms, the u oscillator starts to oscillate, and the v oscillator is forced to move via their mutual coupling ξ. The oscillating u and v oscillators act as secondary sources and emit electromagnetic waves polarized along x and y directions, respectively. This consequently results in output polarization azimuth different from the x direction, i.e., polarization rotation happens. Furthermore, when the oscillators are arrayed, they are mutually coupled via their in-plane electromagnetic radiation. Considering the transverse nature of the electromagnetic waves, the nth u (or v) oscillator would only be influenced by the emission from the u (or v) oscillators of the neighbors (m), which we describe here using a coupling coefficient $\Gamma_{u,m}$ (or $\Gamma_{v,m}$). Thus, the displacements U_n and V_n in the nth meta-atom could be elucidated by

$$\ddot{U}_n + \gamma_u \dot{U}_n + \omega_u^2 U_n + \xi V_n + \sum_m \Gamma_{u,m} U_m = -\frac{e_u}{m_u} E_x e^{-i\omega t},$$
$$\ddot{V}_n + \gamma_v \dot{V}_n + \omega_v^2 V_n + \xi U_n + \sum_m \Gamma_{v,m} V_m = 0. \quad (1)$$

Considering the periodic boundary condition between the meta-atoms and the normal light incidence, the oscillator displacements in each unit cell are identical. Thus, we could rewrite as $\sum_m \Gamma_{u,m} U_m = \Gamma_u U_n$ and $\sum_m \Gamma_{v,m} V_m = \Gamma_v V_n$, where $\sum_m \Gamma_{u,m} = \Gamma_u$ and $\sum_m \Gamma_{v,m} = \Gamma_v$ denote the equivalent total interactions from all the neighbors to the nth one. Hence the displacements and their mutual phase difference could be yielded by solving above linear differential equations as

$$U_n = \frac{e_u}{m_u} \frac{E_x(\omega^2 + i\gamma_v\omega - \omega_v^2 - \Gamma_v)}{(\omega^2 + i\gamma_u\omega - \omega_u^2 - \Gamma_u)(\omega^2 + i\gamma_v\omega - \omega_v^2 - \Gamma_v) - \xi^2} e^{-i\omega t},$$
$$V_n = \frac{e_u}{m_u} \frac{E_x \xi}{(\omega^2 + i\gamma_u\omega - \omega_u^2 - \Gamma_u)(\omega^2 + i\gamma_v\omega - \omega_v^2 - \Gamma_v) - \xi^2} e^{-i\omega t},$$
$$\delta = \arctan\left(\frac{-\gamma_v \omega}{\omega^2 - \omega_v^2 - \Gamma_v}\right). \quad (2)$$

The amplitude ratio $(|V_n|/|U_n|)$ together with δ determine the polarization azimuth of the radiated fields from the oscillator array:

$$\phi = \frac{1}{2}\arctan\left(\frac{2(|V_n|/|U_n|)\cos\delta}{1 - (|V_n|/|U_n|)^2}\right). \quad (3)$$

In this work, the 90° rotation of the x-polarized incidence leads to the output polarization along the y direction. This demands $\delta = \pm\pi/2$ and $|V_n| > |U_n|$ according to the Jones calculus. The first condition requires the resonant oscillation of v to make it lag behind the u actuation by $\pi/2$. This is satisfied mathematically by zeroing the denominator in δ [Eq. (2)], implying a resonance shift of v to $\omega_c = \sqrt{\omega_v^2 + \Gamma_v}$ as a result of inter-meta-atom coupling. Furthermore, the second condition, which asks for the stronger $|V_n|$ than its driving source $|U_n|$, can only be fulfilled in the chiral system showing different v and u parameters. Meanwhile, the ξ needs to be larger than $\gamma_v\sqrt{\omega_v^2 + \Gamma_v}$ to generate a sufficient driving force from u to v. For a given group of $(\omega_u, \gamma_u, \omega_v, \gamma_v)$, the response of the system is dependent on the Γ_v. Figure 1(c) presents the phase diagram of the ϕ as functions of Γ_v and ω. The value of ϕ is normalized to the domain of $(-90°, +90°]$. It is clear that ϕ could achieve 90° when Γ_v is smaller than a threshold value of $\Gamma_c = \xi^2/\gamma_v^2 - \omega_v^2$ and at the ω_c. The relationship between ϕ and ω for different Γ_v values is given in Fig. 1(d). It is shown that the ϕ cannot exceed 45° for $\Gamma_v > \Gamma_c$, but achieves 90° when $\Gamma_v \le \Gamma_c$. We define the maximum achievable optical rotation $|\phi|_{\max}$ from the array as an order parameter, and its dependence on the Γ_v is shown in Fig. 1(e). Indeed $|\phi|_{\max}$ shows a phase transition and changes from 45° to 90° abruptly at Γ_c (Supplemental Material [59] gives detailed explanation). Consequently, two distinct phases ("I" and "II") can be defined depending on whether $|\phi|_{\max}$ achieves 90° or not. Considering that the ϕ is related to the U_n and V_n [Eq. (3)], which are proportional to the first-order derivative of total energy (the sum of potential and kinetic energies) of the oscillator array, the phase transition here could be classified as the first-order transition, following the Ehrenfest classification scheme [65].

The "L"-shaped metamaterial samples were fabricated using focused ion beam milling through a 100 nm thick gold film deposited on a fused quartz substrate. The meta-atoms are periodically arranged in a square lattice, whose period P varies for different metamaterial arrays. The typical SEM image of a single meta-atom with $P = 300$ nm is shown in Fig. 1(a). The optical rotations of the metamaterials were studied using a finite-element method (COMSOL). The optical constant of gold is described by data from Ref. [66]. The refractive index of the substrate was set as 1.45. Periodic conditions were applied on the boundaries between meta-atoms. Inside the geometry, continuity conditions are imposed everywhere, except that scattering boundary conditions were applied to the boundaries where the wave is entering and outgoing the structure. Figure 2(a) presents the simulated spectra of the ϕ for metamaterials with P ranging from 410 to 450 nm. We summarize the $|\phi|_{\max}$ for various P in Fig. 2(b). Agreeing with the prediction from the coupled-oscillator model $|\phi|_{\max}$ increases for larger P, which corresponds to the decreased Γ. And $|\phi|_{\max}$ suffers the abrupt transition from 45° to 90° when P reaches a critical value of 416 nm, showing a similar feature as Fig. 1(d). These consistences validate our proposed phase transition coupled-oscillator model. Furthermore, we found that when P is larger than 628 nm, the metamaterials return to phase II again, which could be attributed to the decreased ξ in the meta-atom as the wavelength increases.

In the experiment, a supercontinuum laser (6W-SC-Pro, YSL Photonics) was adopted as a broadband light source,

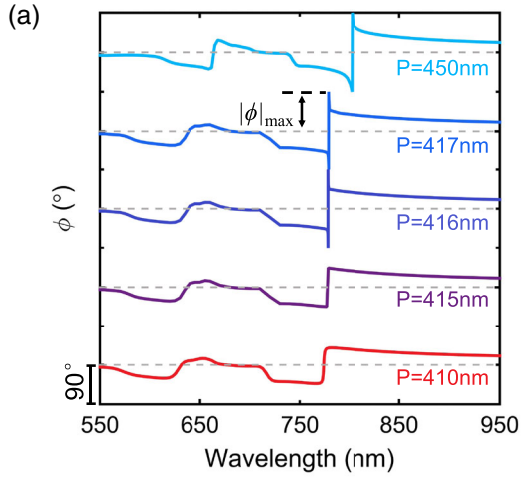

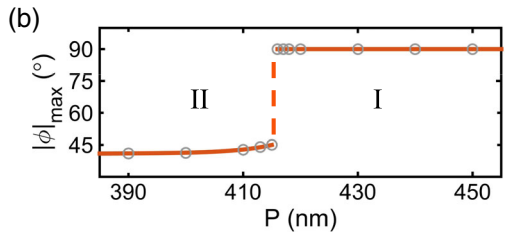

FIG. 2. Simulated optical rotation spectra. (a) ϕ spectra for metamaterial arrays with various periods. For structures with P larger than 416 nm, the ϕ achieves 90°. The curves are shifted vertically for clarity of presentation. Vertical scale is shown in bottom-left corner. Gray dashed lines show zero level of each ϕ curve. (b) The $|\phi|_{max}$ as a function of P, which shows a discontinuous transition at 416 nm. The empty circles are the simulated data, and solid lines are guides for the eye.

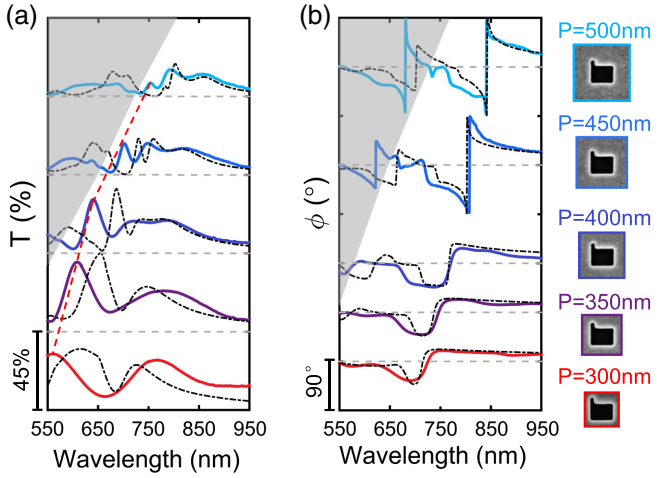

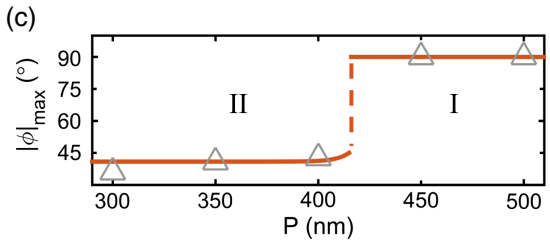

FIG. 3. Experimental characterization of metamaterials' performance. (a) Transmission spectra for metamaterials with P changes from 300 to 500 nm in a step of 50 nm under x-polarized incident light. Experimental and simulated results are given in solid and dashed lines, respectively. The spectra are shifted vertically for clarity of presentation. Scale bar of 45% is shown in bottom-left corner. Gray dashed lines give zero transmission level for each curve. (b) Experimental (solid lines) and simulated (dashed lines) ϕ for metamaterials. Vertical scales are shown in bottom-left corner. Gray dashed lines show the zero level of each ϕ curve. The experimental and simulated results show reasonable agreement except in the shadowed ranges, where optical diffraction happens. The SEM images of unit cells are shown on the right. (c) Comparison between the experimental and the simulated $|\phi|_{max}$ as a function of P. Empty triangles are the experimental data, and solid lines are the simulated result replotted from Fig. 2(b). The $|\phi|_{max}$ achieves 90° for P of 450 and 500 nm, which are much larger than the transition threshold of 416 nm.

whose output light was polarized along the x direction using a Glan-Taylor (GT) calcite polarizer. We used a ×10 objective (0.3 NA) for illumination and another ×100 objective (0.9 NA) for collection. Transmission spectra of the metamaterials referenced to the naked fused quartz substrate were characterized by a spectrometer. Experimental and simulated results are given in solid and dashed lines in Fig. 3(a), respectively. As P increases from 300 to 500 nm in a step of 50 nm, the spectral resonances suffer redshift as indicated by the red dashed line, and the transmittance decreases slightly due to the lower aperture ratio of the meta-atoms (shown by SEM images on the right). The optical rotation spectra of the metamaterials were measured using a homebuilt polarimeter, consisting of a rotating achromatic quarter-wave plate (WP), GT polarizer, and a fiber coupled spectrometer. The experimental and simulated results are shown by solid and dashed lines in Fig. 3(b), respectively (circular polarization extinction ratio spectra are given in Supplemental Material [59]). In shadowed regimes, the metamaterial periods P are larger than the wavelengths in the substrate, thus nonzero-order optical diffraction happens. We will not discuss the properties in these spectral regions, because interference between the diffraction orders complicates the polarization analysis, and deteriorates the real application convenience. For wavelength range beyond the shadows, only zero-order transmission occurs. It could be seen that when P increases, the spectra shift down in frequency, and the ϕ increases. The ϕ are less than 45° for $P = 300$ to 400 nm, which are in the phase II indicated in Fig. 2(b). For the $P = 450$ and 500 nm, which are much larger than the threshold of 416 nm, ϕ achieve 90°, and the metamaterials transform into the phase I. Such phase transition behavior is intuitively shown in Fig. 3(c). The experimental results agree reasonably well with the simulated ones in Fig. 3. And discrepancies between them can be mainly attributed to differences between the simulation models and the real

samples, for example side walls of L-shaped holes were assumed to be vertical in the simulations rather than inclined as the real sample.

In conclusion, we have reported a phase-transition optical activity from the single layer chiral metamaterials. We developed a phase-transition coupled-oscillator array model to elucidate the physical behaviors of the metamaterials, in which both the intra- and inter-meta-atom interactions are taken into consideration. The couplings between the meta-atoms, which can be tuned easily by changing the P of metamaterials, are proved to play important roles in inducing the phase transition of the metamaterials and also in influencing the ϕ level. By reducing the inter-meta-atom coupling below the critical strength (equivalent to increasing the P above a threshold value), the maximum optical rotation from the single layer metamaterial can be abruptly switched from below 45° to 90°. Our findings, from a fundamental point of view, provide a new angle in understanding and boosting the chiro-optical interactions, which benefit improving the sensitivity of chiro-optical spectroscopy for determining the purity of chemicals, and can be applied in manufacturing ultracompact chiral polarization components for displays to telecommunications *et al.* Furthermore, it is expected that our results could open a new door for a variety of researches and applications in the field of phase-transition photonics.

This work was supported by National Key R&D Program of China (2017YFA0305100, 2017YFA0303800); National Natural Science Foundation of China (92050114, 61775106, 11904182, 11711530205, 11374006, 11774185, 91750204); the 111 Project (B07013); PCSIRT (IRT0149); the Open Research Program of Key Laboratory of 3D Micro/Nano Fabrication and Characterization of Zhejiang Province; the Fundamental Research Funds for the Central Universities (010-63201003, 010-63201008, and 010-63201009); the Tianjin youth talent support program. We thank the Nanofabrication Platform of Nankai University for fabricating samples.

*ren_mengxin@nankai.edu.cn
†jjxu@nankai.edu.cn

[1] M. Hentschel, M. Schäferling, T. Weiss, N. Liu, and H. Giessen, Three-dimensional chiral plasmonic oligomers, Nano Lett. **12**, 2542 (2012).
[2] R. Sarma, L. Ge, J. Wiersig, and H. Cao, Rotating Optical Microcavities with Broken Chiral Symmetry, Phys. Rev. Lett. **114**, 053903 (2015).
[3] T. Nguyen, F. Han, N. Andrejevic, R. Pablo-Pedro, A. Apte, Y. Tsurimaki, Z. Ding, K. Zhang, A. Alatas, E. E. Alp, S. Chi, J. Fernandez-Baca, M. Matsuda, D. A. Tennant, Y. Zhao, Z. Xu, J. W. Lynn, S. Huang, and M. Li, Topological Singularity Induced Chiral Kohn Anomaly in a Weyl Semimetal, Phys. Rev. Lett. **124**, 236401 (2020).
[4] D. F. Arago, Mémoire sur une modification remarquable qu'éprouvent les rayons lumineux dans leur passage à travers certains corps diaphanes et sur quelques autres nouveaux phénomènes d'optique, Mém. Inst. France, Part I **12**, 93 (1811).
[5] L. Pasteur, Recherches sur les propriétés spécifiques des deux acides qui composent l'acide racémique, Ann. Chim. Phys. **28**, 56 (1850).
[6] C. Wu, H. Q. Li, X. Yu, F. Li, H. Chen, and C. T. Chan, Metallic Helix Array as a Broadband Wave Plate, Phys. Rev. Lett. **107**, 177401 (2011).
[7] R. Jones, G. Buonaiuto, B. Lang, I. Lesanovsky, and B. Olmos, Collectively Enhanced Chiral Photon Emission from an Atomic Array near a Nanofiber, Phys. Rev. Lett. **124**, 093601 (2020).
[8] E. W. Meijer, E. E. Havinga, and G. L. J. A. Rikken, Second-Harmonic Generation in Centrosymmetric Crystals of Chiral Molecules, Phys. Rev. Lett. **65**, 37 (1990).
[9] Y. Q. Tang and A. E. Cohen, Optical Chirality and Its Interaction with Matter, Phys. Rev. Lett. **104**, 163901 (2010).
[10] J. Feis, D. Beutel, J. Köpfler, X. Garcia-Santiago, C. Rockstuhl, M. Wegener, and I. Fernandez-Corbaton, Helicity-Preserving Optical Cavity Modes for Enhanced Sensing of Chiral Molecules, Phys. Rev. Lett. **124**, 033201 (2020).
[11] W. L. Gao, M. Lawrence, B. Yang, F. Liu, F. Z. Fang, B. Béri, J. Li, and S. Zhang, Topological Photonic Phase in Chiral Hyperbolic Metamaterials, Phys. Rev. Lett. **114**, 037402 (2015).
[12] M. Xiao, Q. Lin, and S. H. Fan, Hyperbolic Weyl Point in Reciprocal Chiral Metamaterials, Phys. Rev. Lett. **117**, 057401 (2016).
[13] S. Yoo and Q. H. Park, Chiral Light-Matter Interaction in Optical Resonators, Phys. Rev. Lett. **114**, 203003 (2015).
[14] S. Mahmoodian, Chiral Light-Matter Interaction Beyond the Rotating-Wave Approximation, Phys. Rev. Lett. **123**, 133603 (2019).
[15] V. K. Valev, J. J. Baumberg, C. Sibilia, and T. Verbiest, Chirality and chiroptical effects in plasmonic nanostructures: Fundamentals, recent progress, and outlook, Adv. Mater. **25**, 2517 (2013).
[16] M. Hentschel, M. Schäferling, X. Y. Duan, H. Giessen, and N. Liu, Chiral plasmonics, Sci. Adv. **3**, e1602735 (2017).
[17] M. Qiu, L. Zhang, Z. X. Tang, W. Jin, C. W. Qiu, and D. Y. Lei, 3D metaphotonic nanostructures with intrinsic chirality, Adv. Funct. Mater. **28**, 1803147 (2018).
[18] X. Xiong, W. H. Sun, Y. J. Bao, M. Wang, R. W. Peng, C. Sun, X. Lu, J. Shao, Z. F. Li, and N. B. Ming, Construction of a chiral metamaterial with a U-shaped resonator assembly, Phys. Rev. B **81**, 075119 (2010).
[19] Z. F. Li, R. K. Zhao, T. Koschny, M. Kafesaki, K. B. Alici, E. Colak, H. Caglayan, E. Ozbay, and C. M. Soukoulis, Chiral metamaterials with negative refractive index based on four "U" split ring resonators, Appl. Phys. Lett. **97**, 081901 (2010).
[20] M. Mutlu and E. Ozbay, A transparent 90° polarization rotator by combining chirality and electromagnetic wave tunneling, Appl. Phys. Lett. **100**, 051909 (2012).
[21] C. Huang, Y. J. Feng, J. M. Zhao, Z. B. Wang, and T. Jiang, Asymmetric electromagnetic wave transmission of linear

polarization via polarization conversion through chiral metamaterial structures, Phys. Rev. B **85**, 195131 (2012).
[22] K. Hannam, D. A. Powell, I. V. Shadrivov, and Y. S. Kivshar, Dispersionless optical activity in metamaterials, Appl. Phys. Lett. **102**, 201121 (2013).
[23] J. K. Gansel, M. Thiel, M. S. Rill, M. Decker, K. Bade, V. Saile, G. von Freymann, S. Linden, and M. Wegener, Gold helix photonic metamaterial as broadband circular polarizer, Science **325**, 1513 (2009).
[24] J. K. Gansel, M. Wegener, S. Burger, and S. Linden, Gold helix photonic metamaterials: A numerical parameter study, Opt. Express **18**, 1059 (2010).
[25] M. Thiel, M. Decker, M. Deubel, M. Wegener, S. Linden, and G. von Freymann, Polarization stop bands in chiral polymeric three-dimensional photonic crystals, Adv. Mater. **19**, 207 (2007).
[26] H. S. Park, T. T. Kim, H. D. Kim, K. Kim, and B. Min, Nondispersive optical activity of meshed helical metamaterials, Nat. Commun. **5**, 5435 (2014).
[27] S. Vignolini, N. A. Yufa, P. S. Cunha, S. Guldin, I. Rushkin, M. Stefik, K. Hur, U. Wiesner, J. J. Baumberg, and U. Steiner, A 3D optical metamaterial made by self-assembly, Adv. Mater. **24**, OP23 (2012).
[28] S. S. Oh, A. Demetriadou, S. Wuestner, and O. Hess, On the origin of chirality in nanoplasmonic gyroid metamaterials, Adv. Mater. **25**, 612 (2013).
[29] M. Decker, M. Ruther, C. E. Kriegler, J. Zhou, C. M. Soukoulis, S. Linden, and M. Wegener, Strong optical activity from twisted-cross photonic metamaterials, Opt. Lett. **34**, 2501 (2009).
[30] M. Decker, R. Zhao, C. M. Soukoulis, S. Linden, and M. Wegener, Twisted split-ring-resonator photonic metamaterial with huge optical activity, Opt. Lett. **35**, 1593 (2010).
[31] Y. H. Cui, L. Kang, S. F. Lan, S. Rodrigues, and W. S. Cai, Giant chiral optical response from a twisted-arc metamaterial, Nano Lett. **14**, 1021 (2014).
[32] X. H. Yin, M. Schäferling, A. K. U. Michel, A. Tittl, M. Wuttig, T. Taubner, and H. Giessen, Active chiral plasmonics, Nano Lett. **15**, 4255 (2015).
[33] A. Basiri, X. H. Chen, J. Bai, P. Amrollahi, J. Carpenter, Z. Holman, C. Wang, and Y. Yao, Nature-inspired chiral metasurfaces for circular polarization detection and full-stokes polarimetric measurements, Light Sci. Appl. **8**, 78 (2019).
[34] C. M Soukoulis and M. Wegener, Past achievements and future challenges in the development of three-dimensional photonic metamaterials, Nat. Photonics **5**, 523 (2011).
[35] A. Papakostas, A. Potts, D. M. Bagnall, S. L. Prosvirnin, H. J. Coles, and N. I. Zheludev, Optical Manifestations of Planar Chirality, Phys. Rev. Lett. **90**, 107404 (2003).
[36] M. Kuwata-Gonokami, N. Saito, Y. Ino, M. Kauranen, K. Jefimovs, T. Vallius, J. Turunen, and Y. Svirko, Giant Optical Activity in Quasi-Two-Dimensional Planar Nanostructures, Phys. Rev. Lett. **95**, 227401 (2005).
[37] B. F. Bai, J. Laukkanen, A. Lehmuskero, and J. Turunen, Simultaneously enhanced transmission and artificial optical activity in gold film perforated with chiral hole array, Phys. Rev. B **81**, 115424 (2010).
[38] M. X. Ren, E. Plum, J. J. Xu, and N. I. Zheludev, Giant nonlinear optical activity in a plasmonic metamaterial, Nat. Commun. **3**, 833 (2012).
[39] E. Plum, X. X. Liu, V. A. Fedotov, Y. Chen, D. P. Tsai, and N. I. Zheludev, Metamaterials: Optical Activity without Chirality, Phys. Rev. Lett. **102**, 113902 (2009),
[40] M. X. Ren, W. Wu, W. Cai, B. Pi, X. Z. Zhang, and J. J. Xu, Reconfigurable metasurfaces that enable light polarization control by light, Light Sci. Appl. **6**, e16254 (2017).
[41] L. B. Mao, K. Liu, S. Zhang, and T. Cao, Extrinsically 2D-chiral metamirror in near-infrared region, ACS Photonics **7**, 375 (2020).
[42] S. Y. Yang, Z. Liu, S. Hu, A. Z. Jin, H. F. Yang, S. Zhang, J. J. Li, and C. Z. Gu, Spin-selective transmission in chiral folded metasurfaces, Nano Lett. **19**, 3432 (2019).
[43] F. Xie, W. Wu, M. X. Ren, W. Cai, and J. J. Xu, Lattice collective interaction engineered optical activity in metamaterials, Adv. Opt. Mater. **8**, 1901435 (2020).
[44] S. S. Oh and O. Hess, Chiral metamaterials: Enhancement and control of optical activity and circular dichroism, Nano Convergence **2**, 24 (2015).
[45] Z. J. Wang, F. Cheng, T. Winsor, and Y. M. Liu, Optical chiral metamaterials: A review of the fundamentals, fabrication methods and applications, Nanotechnology **27**, 412001 (2016).
[46] S. Yoo and Q. H. Park, Metamaterials and chiral sensing: A review of fundamentals and applications, Nanophotonics **8**, 249 (2019).
[47] R. V. Solé, *Phase Transitions* (Princeton University Press, Princeton, NJ, 2011).
[48] M. Z. Hasan and C. L. Kane, Colloquium: Topological insulators, Rev. Mod. Phys. **82**, 3045 (2010).
[49] L. Q. Cong, P. Pitchappa, C. K. Lee, and R. Singh, Active phase transition via loss engineering in a terahertz mems metamaterial, Adv. Mater. **29**, 1700733 (2017).
[50] A. Hierro, M. M. Bajo, M. Ferraro, J. Tamayo-Arriola, N. L. Biavan, M. Hugues, J. M. Ulloa, M. Giudici, J. M. Chauveau, and P. Genevet, Optical Phase Transition in Semiconductor Quantum Metamaterials, Phys. Rev. Lett. **123**, 117401 (2019).
[51] A. Rahimzadegan, D. Arslan, R. N. S. Suryadharma, S. Fasold, M. Falkner, T. Pertsch, I. Staude, and C. Rockstuhl, Disorder-Induced Phase Transitions in the Transmission of Dielectric Metasurfaces, Phys. Rev. Lett. **122**, 015702 (2019).
[52] L. Lu, J. D. Joannopoulos, and M. Soljačić, Topological photonics, Nat. Photonics **8**, 821 (2014).
[53] M. V. Rybin, D. S. Filonov, K. B. Samusev, P. A. Belov, and M. F. Limonov, Phase diagram for the transition from photonic crystals to dielectric metamaterials, Nat. Commun. **6**, 10102 (2015).
[54] R. El-Ganainy, K. G. Makris, M. Khajavikhan, Z. H. Musslimani, S. Rotter, and D. N. Christodoulides, Non-Hermitian physics and PT symmetry, Nat. Phys. **14**, 11 (2018).
[55] M. Born, Über die natürliche optische aktivität von flüssigkeiten und gasen, Phys. Z. **16**, 251 (1915).
[56] Y. P. Svirko and N. I. Zheludev, *Polarization of Light in Nonlinear Optics* (Wiley-VCH, New York, 2000).
[57] X. H. Yin, M. Schäferling, B. Metzger, and H. Giessen, Interpreting chiral nanophotonic spectra: The plasmonic Born-Kuhn model, Nano Lett. **13**, 6238 (2013).

[58] H. Kurosawa and S. Inoue, Born-Kuhn model for magneto-chiral effects, Phys. Rev. A **98**, 053805 (2018).
[59] See Supplemental Material at http://link.aps.org/supplemental/10.1103/PhysRevLett.125.237401 for more details, which includes Refs. [60–64].
[60] M. A. Ordal, R. J. Bell, R. W. Alexander, L. L. Long, and M. R. Querry, Optical properties of fourteen metals in the infrared and far infrared: Al, Co, Cu, Au, Fe, Pb, Mo, Ni, Pd, Pt, Ag, Ti, V, and W, Appl. Opt. **24**, 4493 (1985).
[61] M. G. Blaber, M. D. Arnold, and M. J. Ford, Search for the ideal plasmonic nanoshell: The effects of surface scattering and alternatives to gold and silver, J. Phys. Chem. C **113**, 3041 (2009).
[62] J. M. McMahon, S. K. Gray, and G. C. Schatz, Nonlocal Optical Response of Metal Nanostructures with Arbitrary Shape, Phys. Rev. Lett. **103**, 097403 (2009).
[63] P. C. Wu, C. Y. Liao, V. Savinov, T. L. Chung, W. T. Chen, Y. W. Huang, P. R. Wu, Y. H. Chen, A. Q. Liu, N. I. Zheludev *et al.*, Optical anapole metamaterial, ACS Nano **12**, 1920 (2018).
[64] M. Bass, C. DeCusatis, J. Enoch, V. Lakshminarayanan, G. F. Li, C. MacDonald, V. Mahajan, and E. Van Stryland, *Handbook of Optics* (McGraw-Hill, New York, 2009).
[65] B. Fultz, *Phase Transitions in Materials* (Cambridge University Press, Cambridge, England, 2020).
[66] P. B. Johnson and R. W. Christy, Optical constants of the noble metals, Phys. Rev. B **6**, 4370 (1972).